Computational investigation of unusual behavior in certain capillary tubes

Victor Brady*, Paul Concus†, and Robert Finn‡

Abstract

We investigate computationally two recent mathematical findings involving unusual behavior of solutions of the Young-Laplace capillary equation in cylindrical tubes of particular sections. The first concerns a configuration for which smoothing of the boundary curve at a sharp corner leads from existence to non-existence of a solution over the container section in zero gravity. The second describes a discontinuous behavior of relative rise height in nesting tubes placed vertically in an infinite reservoir. The numerical results support and quantify the mathematical predictions.

1 Introduction

The free surface of a liquid partly filling a container can behave in curious unexpected ways. We investigate computationally recent mathematical results for two examples of such behavior under reduced gravity. The first example describes behavior of a liquid in a cylindrical container whose section has a corner: In the absence of gravity, smoothing of the corner can transform a situation for which a solution of the governing Young-Laplace equations exists and is bounded to one for which no solution exists, contrary

*Lawrence Berkeley National Laboratory, Berkeley, CA 94720

†Lawrence Berkeley National Laboratory and Department of Mathematics, University of California at Berkeley, Berkeley, CA 94720

‡Department of Mathematics, Stanford University, Stanford, CA 94305

to what one would customarily expect. The second example concerns rise height of a liquid in capillary tubes dipped into an infinite reservoir in a vertically downward gravity field: Again contrary to what one might expect, smaller tubes do not always lift wetting liquids higher than do larger ones; moreover even in simple configurations the height relationship can reverse with arbitrarily large jump for small changes in tube section.

Our study is based on the classical Laplace-Young equations for an equilibrium capillary free-surface. For liquid in a vertical cylindrical container of section Ω with a gravity field, if present, that is downward-acting ($B \geq 0$) there holds [1, Sec.1.9] (see Figure 1)

$$\text{div } Tu = Bu + 2H \quad \text{in} \quad \Omega, \qquad Tu = \frac{\nabla u}{\sqrt{1+|\nabla u|^2}}, \tag{1}$$

$$\nu \cdot Tu = \cos\gamma \quad \text{on} \quad \Sigma. \tag{2}$$

The equations have been written in dimensionless form with u being the ratio of height of the liquid-vapor interface to a characteristic length a; $B = \rho g a^2/\sigma$ is the Bond number, with ρ the density difference across the interface, σ the interfacial surface tension, and g the acceleration due to gravity; Σ is the boundary of Ω, and ν is the outward unit normal on Σ; γ denotes the contact angle between the liquid and the wall of the tube. We consider here the case of a wetting liquid $0 \leq \gamma < \frac{\pi}{2}$. (The non-wetting case can be treated analogously.)

For the first problem, for which $B = 0$, the constant $2H$ is determined by the contact angle boundary condition and the container geometry, as

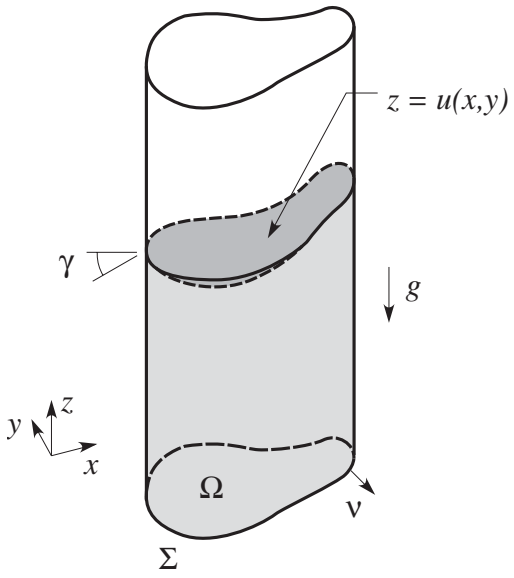

Figure 1: Partly filled cylindrical tube with section Ω.

obtained by integrating (1) by parts over Ω

$$2H = \frac{|\Sigma| \cos\gamma}{|\Omega|}, \tag{3}$$

where $|\Omega|$ and $|\Sigma|$ denote respectively the area and length of Ω and Σ. H is the (constant) mean curvature of the solution surface. For the second problem, for which gravity is present and surface heights are measured from the height at infinity of the reservoir into which the tubes are dipped, the value of H is zero.

2 First Problem

2.1 The Problem

It is generally known that for sufficiently small contact angle in the absence of gravity ($B = 0$), solutions of (1),(2),(3) do not exist in containers with

corners. If α is the smallest interior half-angle at a corner, then the contact angle of a wetting liquid must satisfy the "corner condition" $\alpha + \gamma \geq \pi/2$ for a solution to exist [2]. The range of values of γ for which solutions do exist when $\gamma \geq \pi/2 - \alpha$ depends on the geometry of the entire container section. In familiar cases, rounding of corners increases the range of contact angles for which solutions exist (see, e.g., [3]).

The example of a cylinder with rectangular section is studied in [3]. For the rectangular cylinder one has $\alpha = \pi/4$, and it can be shown that, no matter what the aspect ratio of the rectangle, solutions exist if and only if $\gamma \geq \gamma_{cr}$, where $\gamma_{cr} = \pi/2 - \alpha = \pi/4$. Rounding all corners with rounding radius $\epsilon > 0$ decreases the critical contact angle γ_{cr}. The computed graphs in [3] indicate that, as ϵ increases, the critical contact angle decreases monotonically until the value zero is reached; the specific rounding radius for which the critical contact angle is zero (i.e., a solution exists for all values of γ) depends on the aspect ratio of the rectangle. The results correspond to what one usually expects intuitively: that rounding of corners moderates their effect in inducing singular behavior and increases the range of contact angles over which solutions are possible.

In a recent study [4] it was shown mathematically that the contrary situation can occur. For a certain container, rounding a corner actually results in an increase in critical contact angle. The section of the cylindrical container studied there as an example is shown in Figure 2. The indicated domain is obtained by starting with a quadrilateral circumscribing the unit

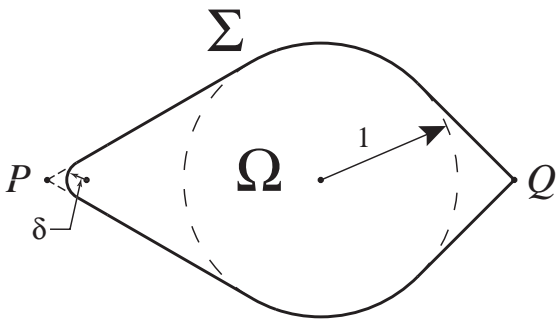

Figure 2: Domain with corner at P rounded by a circular arc of radius δ.

circle and replacing the top and bottom corners by arcs of the inscribed circle. For the example, the remaining corners at P and Q have interior angles 60° and 90°, respectively. The corner at P is then rounded with a circular arc of radius δ, as indicated.

For the underlying, unrounded quadrilateral it can be shown that the corner condition for the smallest interior half-angle, $\alpha = 30^\circ$ at P, determines the critical angle. Thus for the quadrilateral $\gamma_{cr} = 60^\circ$; solutions of (1),(2),(3) are not possible if $\gamma < 60^\circ$, but exist for $\gamma \geq 60^\circ$. Replacing the top and bottom corners by arcs of the inscribed circle does not affect this critical angle.

For the container depicted in Figure 2 the critical value of γ is less than its value of 60° for the corner at P unrounded ($\delta = 0$). This result can be obtained following a general procedure given in [1, Sec. 6.7], [3]. The procedure requires that circular arcs Γ of radius $(|\Sigma| \cos\gamma)/|\Omega|$ be placed in Ω meeting Σ in angles γ (the prescribed contact angle), partitioning off one or more subdomains $\Omega^{'}$ with boundaries $\Sigma^{'}$; see Figure 3. (If Σ has re-entrant corners, a situation we do not consider here, separate corner conditions are

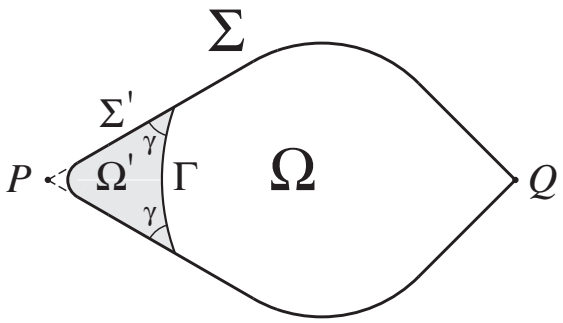

Figure 3: Domain Ω partitioned by a circular arc Γ meeting Σ in angles γ.

required.) For all possible placements of Γ, one determines the sign of the functional $\Phi(\Omega; \Gamma; \gamma)$ defined by

$$\Phi \equiv |\Gamma| - |\Sigma^{'}| \cos\gamma + 2H|\Omega^{'}|, \tag{4}$$

where $2H$ is given by (3). Then the procedure yields the result that a solution of (1),(2),(3) exists if and only if Φ is positive for all such arcs Γ. It turns out that for many domains of practical interest there are only a few configurations that need to be considered.

The configuration depicted in Figure 3 is proved to be the critical one for the particular value of the rounding radius δ at P that corresponds to $\gamma_{cr} = 59°$. That is, for this configuration as γ decreases from values larger than $59°$ the sign of Φ changes from positive to negative as γ passes through the value $59°$, but it remains positive for other possible configurations of Γ. (It can be shown similarly that if the corner at P is unrounded ($\delta = 0$), then for the critical value $\gamma = \gamma_{cr} = 60°$ the particular arc Γ in Figure 3 is no longer interior to Ω but passes through P; for the other possible configurations of Γ, Φ remains positive.) See [4] for details; see also [3]

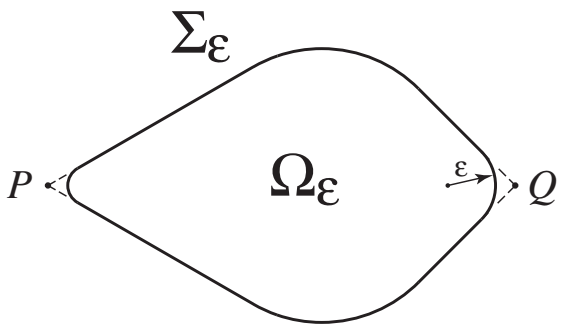

Figure 4: Domain with corner at Q rounded by a circular arc of radius ϵ.

for application of the procedure to other examples, with full details for the rounded rectangle. As a formal solution of the equations, the liquid rises unboundedly in the cut-off subregion Ω' when $\gamma \leq \gamma_{cr}$.

It is shown in [4] that subsequent rounding of the corner at Q (Figure 4) can actually increase the critical angle. This rounding yields the interesting effect of the liquid rising indefinitely at the opposite side of the container, near P, as a result of smoothing the corner Q.

2.2 Computation of effect of rounding

To investigate computationally the predictions in [4], we compute, using the software package MATLAB [5], the amount by which the critical contact angle is increased for the domain in Figure 2 by subsequent rounding of the corner Q, as in Figure 4. We consider values from a range of roundings δ at P in Figure 2 giving rise to domains having critical angle between 45° and 60°. (For smaller contact angles the local effects of the corner at Q would come into play, altering the phenomenon we are studying.) The amount of

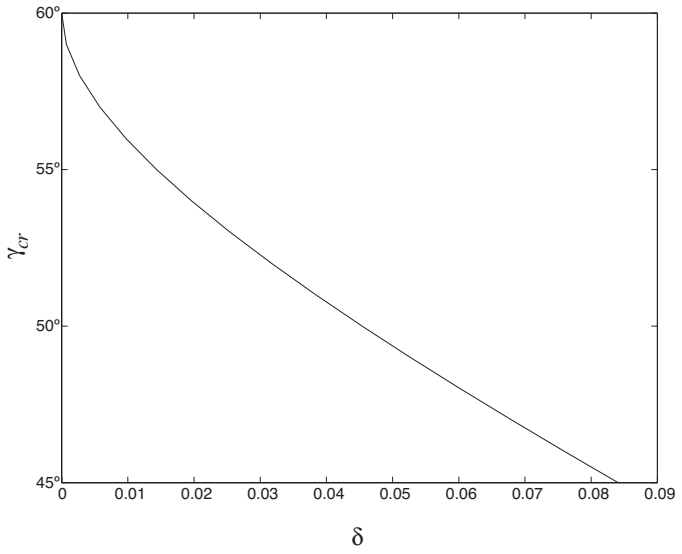

Figure 5: Critical γ vs. rounding radius δ for domain in Figure 2.

rounding at P needed to achieve these critical contact angles is quite small, as depicted in Figure 5. For each value of rounding at P we allow values from the entire range of roundings at Q, from $\epsilon = 0$ (no rounding) to $\epsilon = 1$ (replacing the corner at Q with the arc of the inscribed unit circle). In all cases we calculate from (4) for what value of γ the value of Φ is zero for the configuration of Γ depicted in Figure 3.

The results are illustrated in Figure 6, in which the difference $\gamma_{cr}(\epsilon) - \gamma_{cr}(0)$ between the critical value of γ and its critical value for $\epsilon = 0$ is plotted as a function of ϵ for each rounding at P. As one can demonstrate analytically, the value of the critical γ remains at 60° for no rounding at P ($\delta = 0$) no matter what the rounding $0 \leq \epsilon \leq 1$ is at Q. Thus the curve for $\gamma_{cr} = 60^\circ$ would coincide with the ϵ axis in Figure 6. For increasing rounding at P, the effect of rounding at Q is seen to become increasingly pronounced, with largest effect about midway in the range $0 \leq \epsilon \leq 1$.

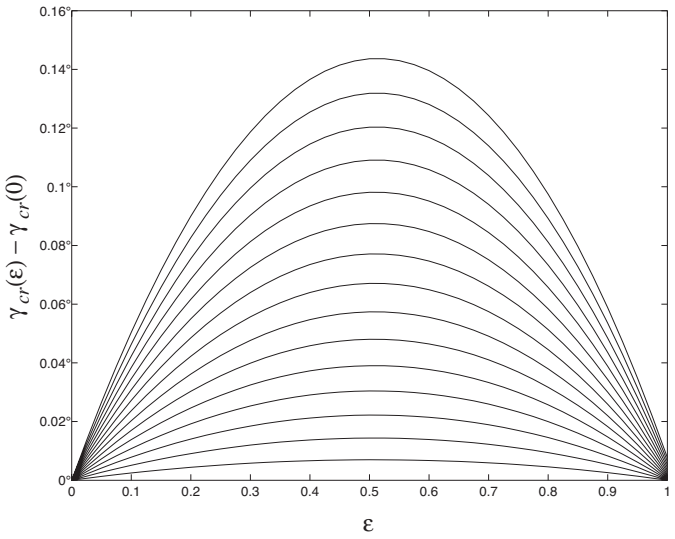

Figure 6: Change in critical γ vs. rounding radius ϵ for domain in Figure 4. The curves from bottom to top are for roundings at P corresponding to $\gamma_{cr}(0) = 59°, 58°, 57°, ..., 45°$, respectively.

For each of the values of $\gamma_{cr}(0)$ corresponding to the curves in Figure 6, we calculated also the value of Φ for all other possible configurations of Γ, which are depicted in [4]. The value of Φ was positive for these other configurations, confirming that the configuration of Figure 3 is the one that yields the critical value for γ when Φ is zero. For roundings at P giving rise to critical angle $\gamma_{cr}(0)$ less than 45°, other configurations of Γ would come into play, connected with local behavior at Q.

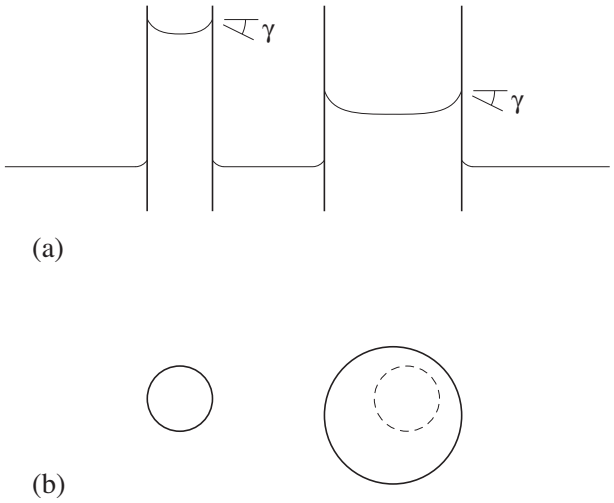

Figure 7: (a) Circular capillary tubes of differing diameters dipped into a reservoir of wetting liquid ($0 \leq \gamma < \pi/2$). (b) At each point of the narrower tube's section liquid rises higher than it does in the wider tube over the same section (dashed subdomain).

3 Second Problem

3.1 The Problem

For capillary tubes of circular section, a narrower tube when dipped vertically into an infinite reservoir raises a wetting liquid higher than does a wider tube (Figure 7(a)). Specifically, the surface height in the narrower tube at each point of its section is greater than the corresponding surface height in the wider tube at each point of a subsection congruent to the section of the smaller tube (Figure 7(b)); this is so even if the smaller section is not placed concentric with the larger one.

For tubes of general section, however, liquid need not rise higher in

a smaller section than in a larger one. This phenomenon is discussed in [6], [1, Sec. 5.3], where a number of criteria are established for the smaller section lifting liquid higher, and in [7],[1, Sec. 5.4], where special cases for the opposite situation are distinguished. It was shown recently [8] that even for sections of simple form the larger tube can lift liquid higher in low-gravity configurations, with the height differences becoming arbitrarily large as gravity decreases to zero. Furthermore, a discontinuous change in behavior can occur for infinitesimal changes in section. In [9] this behavior is investigated computationally for the particular family of nesting rounded-square sections described in [8], for which the sections of all but the smallest tube have discontinuities in curvature. Here we investigate computationally the sections described in [10], for which the interior nesting sections are concentric disks. In this way the curvature discontinuities in the earlier example are eliminated as conceivable source of the singular behavior.

The domains are depicted in Figure 8. According to the mathematical results in [10], the outermost domain can be any polygon, star-shaped with respect to the center of the unit disk, whose sides lie on lines tangent to the disk. In our study, for ease of computation, we have chosen simply Ω_*, the regular such polygon with twelve sides, as indicated in the figure. The smallest domain Ω_1 is the unit disk, and the intermediate domains Ω_t are concentric disks of radius t, $t > 1$, lying interior to the polygon. Our primary interest is in comparing limiting behavior near $t = 1$ among the rise heights for the various domains. Note that if gravity is zero then the lower portion

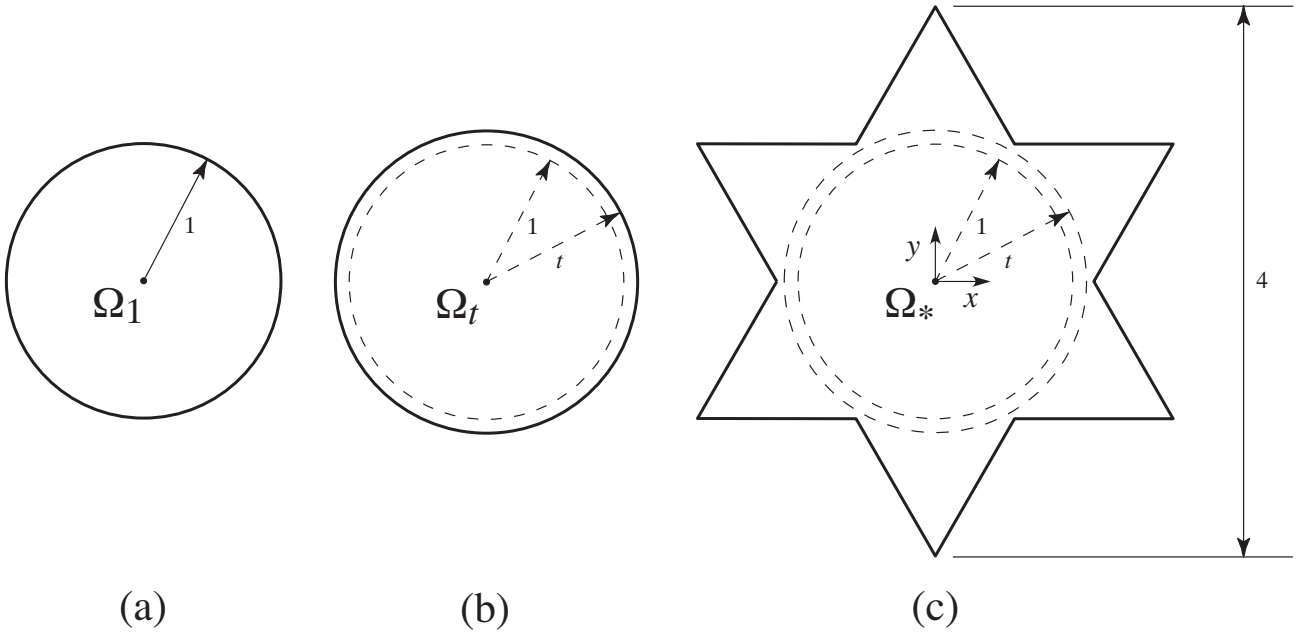

Figure 8: Sections for example problem. (a) unit disk Ω_1, (b) disk Ω_t of radius t, $t > 1$, showing Ω_1 as concentric superimposed dashed subdomain, and (c) polygonal domain Ω_* showing Ω_1 and Ω_t as concentric superimposed dashed subdomains. Extended sides of Ω_* are tangent to the unit circle bounding Ω_1.

of a hemisphere making contact angle γ with the boundary of Ω_1 provides a solution of (1),(2) both for Ω_1 and for the polygonal domain. We restrict γ so as to satisfy requirements for existence of solutions in the polygonal domain, that is $\gamma \geq 60°$.

In [10] the following behavior was found.

> Property (i). *For each of the circular tubes Ω_t, if B is small enough, the polygonal capillary tube Ω_* will raise liquid to a higher level over all of Ω_t than will Ω_t itself. Furthermore, for each fixed t the difference in heights will tend to infinity like $1/B$ as $B \to 0$.*

Thus, in a comparison for small enough B between the polygon and any Ω_t $(t > 1)$, one has that the larger domain (the polygon) lifts liquid higher than does the smaller one, arbitrarily higher as $B \to 0$.

In contrast there holds:

> Property (ii). *For any $B > 0$ the height in the unit disk Ω_1 exceeds at each point of Ω_1 the height for Ω_* and also the height for any of the domains Ω_t.*

Thus, in a comparison between the unit disk Ω_1 and any of the other domains, Ω_t or Ω_*, one has that the smaller domain Ω_1 lifts liquid higher than the larger one, arbitrarily higher in the case of Ω_t. This is the situation no matter how close Ω_t is to being the unit disk Ω_1.

One thus finds that, having chosen any B small enough so that Property (i) holds for a given domain Ω_t $(t > 1)$ (polygon lifts liquid higher than Ω_t does), the height inequality will nevertheless reverse if, for that fixed B, the disk Ω_t approaches the unit disk Ω_1. That happens no matter how small B is initially chosen. See Figure 9, in which u_1, u_t, and u_* denote respectively the surface heights in Ω_1, Ω_t $(t > 1)$, and Ω_*.

Summarizing the limiting behavior, one has:

> Property (iii). *Although the surface height at a given point is continuous in t at $t = 1$ for each fixed $B > 0$, its limiting behavior as $B \to 0$ changes discontinuously in t at $B = 0$.*

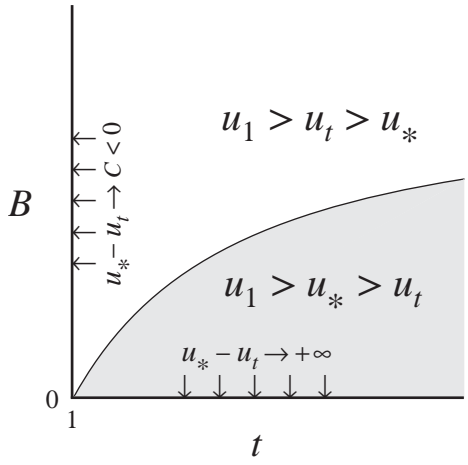

Figure 9: Diagram indicating the subregion (shaded) for which B is small enough for Property (i) to hold. Property (ii) holds for any $B > 0$, for $t > 1$.

We wish to study quantitatively for the domains considered here the manner in which the above behavior occurs. We note that the above results can carry over, with appropriate re-wording, even if t is so large ($t > 2/\sqrt{3}$) that domains Ω_t overlap with Ω_*, or even if Ω_* is actually interior to Ω_t. We focus attention here on the discontinuous behavior as $t \to 1$ and $B \to 0$; correspondingly for our discussion and computations the circular tubes Ω_t are taken to be interior to the polygon as in Figure 8, i.e., $1 < t < 2/\sqrt{3}$. One exception, for $t = 2.1$, will be introduced and discussed at the end of the following subsection.

3.2 Computational results for second problem

To compute the surface heights $u(x, y)$ in the various domains we used the software package PLTMG [11] for obtaining numerical solutions of (1),(2) (with $H = 0$, as discussed in Sec. 1). For very small values of B, in which

we are interested, the problem is ill-conditioned, in the same manner as described in [9] for the domains studied there. Surface heights, which grow like $1/B$, can be very large, and the near-singularity can manifest itself as ill-conditioning of the discretized problem. We utilize here the procedures of [9, Secs. III and IV.A] to overcome the difficulties associated with the ill-conditioning and the growth of surface heights. See [9] for details.

The average surface height $\bar{u}$, as obtained from (1),(2) by integration by parts, is $\bar{u} = (|\Sigma| \cos\gamma)/(B|\Omega|)$. Thus for given B and γ the average surface heights depend only on $|\Sigma|/|\Omega|$. It is the difference in this quantity among the various domains, magnified as B becomes small, that underlies much of the striking behavior. For both the unit disc Ω_1 and the polygonal domain Ω_* the value is $|\Sigma|/|\Omega| = 2$. For the domains Ω_t the value is $2/t$.

Equilibrium free-surface configurations were calculated for domains Ω_1, Ω_*, and Ω_t with $t = 1.025, 1.05, ..., 1.15$, for four values of Bond number $B = 100,\ 1,\ 0.01,\ 0.0001$, and for contact angle $\gamma = 70°$. In general, the *a posteriori* error estimates on the meshes used for the domains (approximately 32,000 vertices) indicated accuracies in the solutions of about three or four decimal places.

The numerical results for the test problems are illustrated in Figures 10 and 11. In Figure 10 the liquid surface height difference between Ω_* and Ω_t at their center, denoted by $u_*(0,0) - u_t(0,0)$, is shown for each of the values of B and t (including, for $t = 1$, the height difference between Ω_* and Ω_1). The tabular values are connected with piecewise cubic splines. The

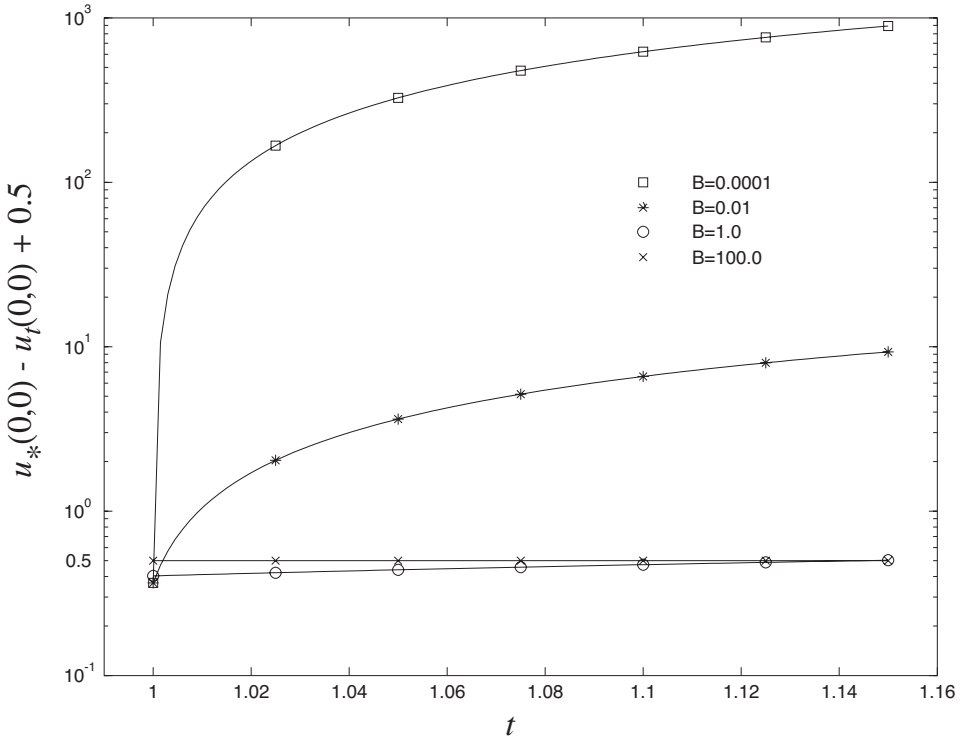

Figure 10: Surface height differences between Ω_* and Ω_t at their centers vs. t for several values of Bond number B.

ordinate is plotted on a logarithmic scale, to take account of the greatly changing behavior that occurs among the values of B, and to bring out the singular nature of the transition to the unit disk. The indicated increment upward by 0.5 allows the negative values of $u_*(0,0) - u_1(0,0)$ to be displayed conveniently on the graph.

In accordance with Properties (i)–(iii) the polygon lifts liquid higher at its center than do the $t > 1$ circular domains Ω_t for small enough B, but does not lift liquid higher than the unit disk Ω_1 (negative values of $u_*(0,0) - u_1(0,0)$). As B decreases, the height differences get very large. The large slope near the end point $t = 1$ as B gets close to zero suggests the discontinuous limiting behavior there.

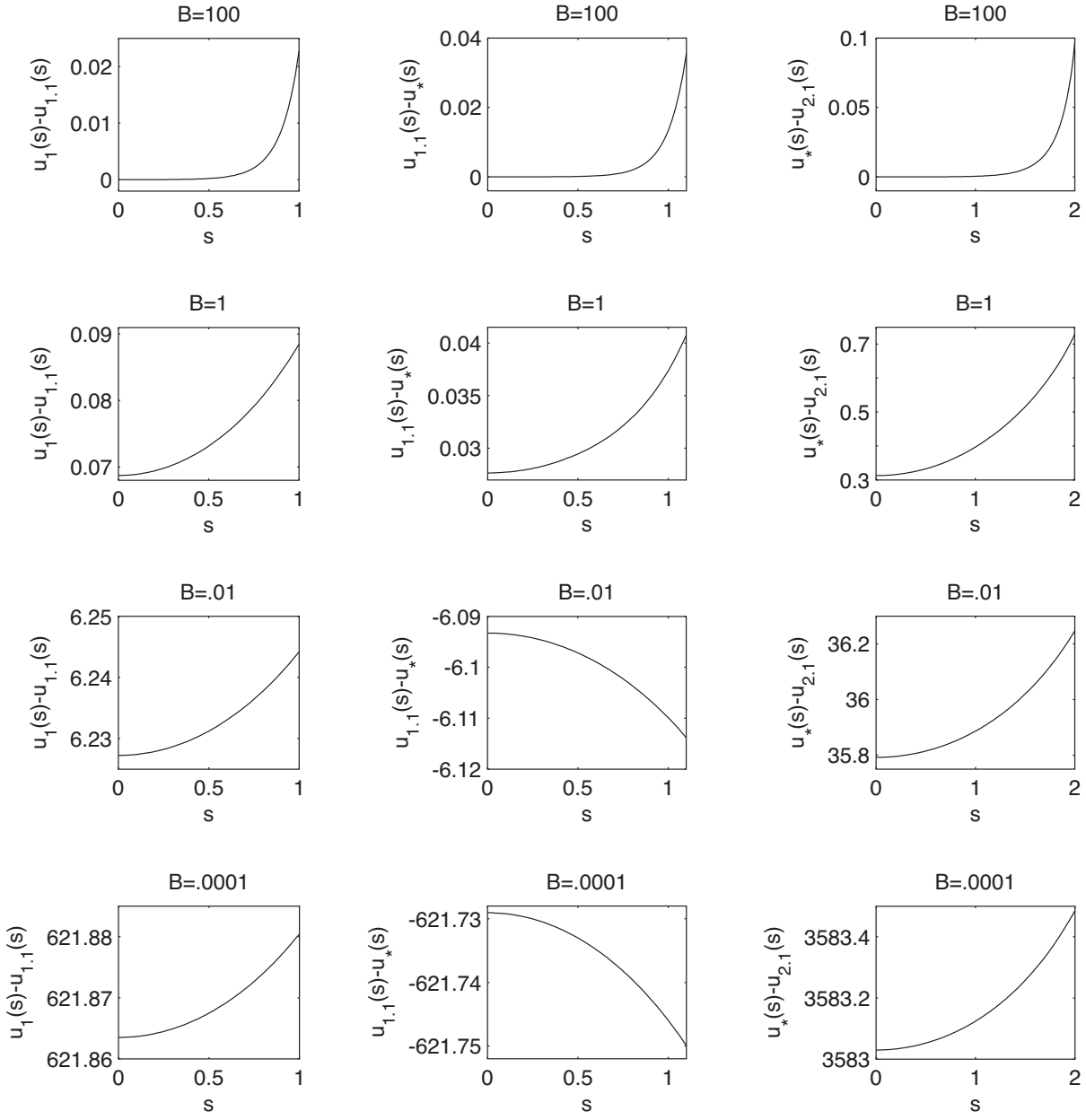

Figure 11: Surface height differences between Ω_1 and $\Omega_{1.1}$ (first column), $\Omega_{1.1}$ and Ω_* (second column), Ω_* and $\Omega_{2.1}$ (third column). $B = 100, 1, 0.01, 0.0001$.

Figure 11 depicts the surface height difference between particular pairs of tubes, as a function of distance s from the common center to the boundary of the superimposed smaller tube, for the indicated Bond numbers. The first column gives the height difference $u_1(s) - u_{1.1}(s)$ between the tubes with section Ω_1 and $\Omega_{1.1}$, with s measured along the radius $y = 0$ (see Figure 8). These values are all positive, in accord with Property (ii) and the diagram in Figure 9; the height difference grows as B decreases, becoming very large for the smallest value of B. The second column gives the height difference $u_{1.1}(s) - u_*(s)$ between $\Omega_{1.1}$ and Ω_*, as measured along the radius $y = 0$. The negative value (larger tube lifts liquid higher) for small-enough B (in this case for the values $B = 0.01$ and $B = 0.0001$), and the large values for the smallest B, are in accord with Property (i) and the diagram in Figure 9.

The third column of Figure 11 gives the computed values of $u_*(s) - u_{2.1}(s)$, the height difference between tubes with section Ω_* and $\Omega_{2.1}$, as measured along a ray $x = 0$. In this case the polygon is interior to the disk. The positive sign of the entries illustrates a result that if the larger domain is a disk the smaller domain always lifts liquid higher, no matter what its shape [1, Sec. 5.4]. The height inequalities become very large as $B \to 0$, reflecting the larger difference between $|\Sigma|/|\Omega|$ for this pair of domains than for the others.

4 Concluding Remarks

The computational results have corroborated and illustrated quantitatively some phenomena uncovered recently in mathematical studies. These phenomena are among the list of striking behaviors that continue to be found for fluid interfaces in reduced gravity.

Acknowledgments

Part of this work was supported by the National Science Foundation under Grants DMS-0103954 and DMS-0103937 and was carried out with computing facilities supported by the Office of Science of the U.S. Department of Energy under Contract DE-AC03-76SF00098. The third author wishes to thank the Max-Planck-Institut für Mathematik in den Naturwissenschaften, in Leipzig, for the hospitality extended him during this investigation.

References

[1] *Finn, R.:* Equilibrium Capillary Surfaces. Springer-Verlag, New York (1986); Russian translation, Mir Publishers, Moscow (1988)

[2] *Concus, P., Finn, R.:* On capillary free surfaces in the absence of gravity. Acta Math. vol. 132, pp. 177–198 (1974)

[3] *Concus, P., Finn, R.:* Dichotomous behavior of capillary surfaces in zero gravity. Microgravity Sci. Technol. vol. 3, pp. 87–92 (1990). Corrigenda of printing errors: vol. 3, p. 230 (1991)

[4] *Finn, R.:* A curious behavior of capillary surfaces. Ann. Univ. Ferrara Sez. VII (N.S.) vol. 48, pp. 153–163 (2002)

[5] MATLAB. Licensed software, The Mathworks Inc., Natick, MA, USA `http://www.mathworks.com`

[6] *Siegel, D.:* Height estimates for capillary surfaces. Pacific J. Math. vol. 88, pp. 471–516 (1980)

[7] *Concus, P., Finn, R.:* On the height of a capillary surface. Math. Zeit. vol. 147, pp. 93–95 (1976)

[8] *Finn, R., Kosmodem'yanskii, A.A., Jr.:* Some unusual comparison properties of capillary surfaces. Pacific J. Math. vol. 205, pp. 119–137 (2002)

[9] *Brady, V., Concus, P., Finn, R.:* Capillary rise in nesting cylinders. Phys. Fluids vol. 15, pp. 1545–1551 (2003)

[10] *Finn, R.:* A new example of singular height transition for capillary surfaces. Calc. Var. Partial Differential Equations vol. 19, pp. 107–115 (2004)

[11] *Bank, R.E.:* PLTMG: A Software Package for Solving Elliptic Partial Differential Equations, Users' Guide 8.0. SIAM, Philadelphia (1988). Software available via Netlib at `http://www.netlib.org/pltmg`